Seventh Aerodynamics Prediction Challenge (APC-7)
2021/06/30, Online

1A18: Aerodynamic Analysis of NASA-CRM at Low Speed and High Angle of Attack conditions Using Hierarchical Cartesian Mesh and Immersed Boundary Method

(階層型直交格子と埋め込み境界法を用いた低速・高迎角条件におけるNASA-CRM巡航形態の空力予測)

〇Atsushi Hara, Keisuke Sugaya, Taro Imamura
(The University of Tokyo)

東京大学
THE UNIVERSITY OF TOKYO

Outline

- Background
- Objective
- Computational conditions
  - Numerical methods
  - Immersed boundary method
  - Computational grid
- Results
  - Aerodynamic coefficients
  - Time history
  - Q criterion
- Conclusion

Background

- Development of UTCart for aircraft design.
  - Grid generation + flow simulation.
  - Automatic and robust generation of hierarchical Cartesian grid.
  - Immersed boundary method (IBM) on stair step grids.
  - Compressible RANS/DDES simulation with wall function.

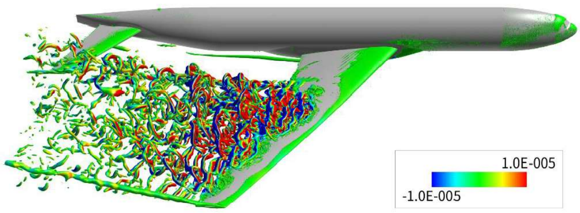

吉永, 菅谷 and 今村, 流力ANSS2020.

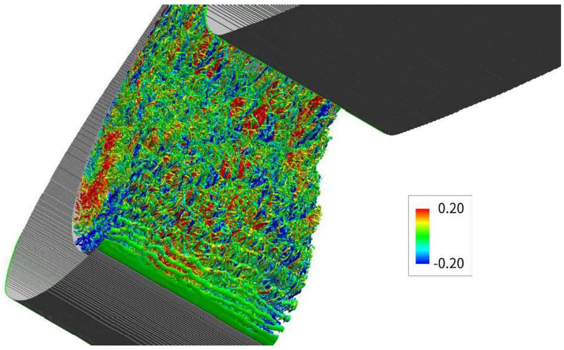

菅谷 and 今村, 流力ANSS2020.

Results of APC-6(1) (IBM)

- A good agreement of aerodynamic coefficients between UTCart and the experiment at low angles of attack (AoA).
- At high AoA, UTCart and the experiment differ.
- **Effects of grid size needs to be investigated.**
- Further study of influence of numerical method is also necessary.

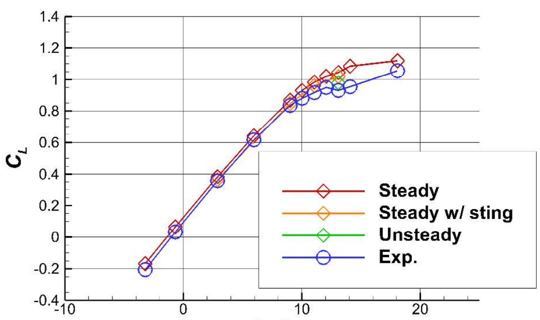

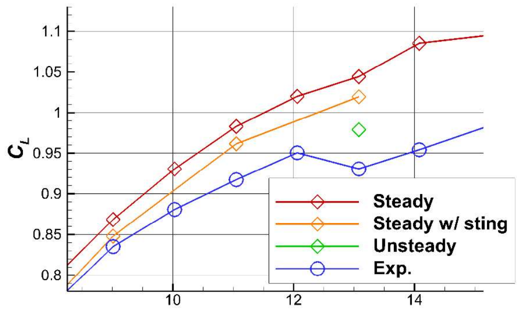

1) Yoshinaga, H., Sugaya, K., and Imamura, T., APC-6, 2020

Objective

- To calculate the NASA-CRM cruising configuration at low speed with finer grids than APC-6 using IBM.
- To investigate the effect of the difference in the grid width of the wake area.
- To assess the prediction accuracy of UTCart for low speed and high AoA simulations.

Numerical method

	Steady	Unsteady
Governing equation	RANS	DDES-p(1)
Turbulence model	SA-noft2-R(2) (Crot = 1)	
Inviscid flux	SLAU + MUSCL ($\kappa = 1/3$)	
Viscous flux	2nd order central difference	
Time integration	MFGS (Local time stepping)	MFGS (Constant dt)
Initial condition	Free-stream	Restart from RANS
Wall boundary condition	IB + SA wall model	
Distance between Image Point and wall (d_{IP})	$2\Delta x$	

1) 玉置 et al., 航空宇宙学会年会, 2018.
2) Dacles-Mariani, j., et al., *AIAA J.*, 1995.

Immersed boundary method

- Flow variables on the Face Center (FC) are calculated from variables on the Image Point (IP) and wall boundary conditions.
- Assuming that tangential velocity is linear between the IP and the wall using wall functions(1).

$$u_{t,FC} = u_{t,IP} - u_{\tau}\left\{\frac{\partial f_{wall}}{\partial y^{+}}(y_{IP}^{+})\right\}(y_{IP}^{+} - y_{FC}^{+})$$

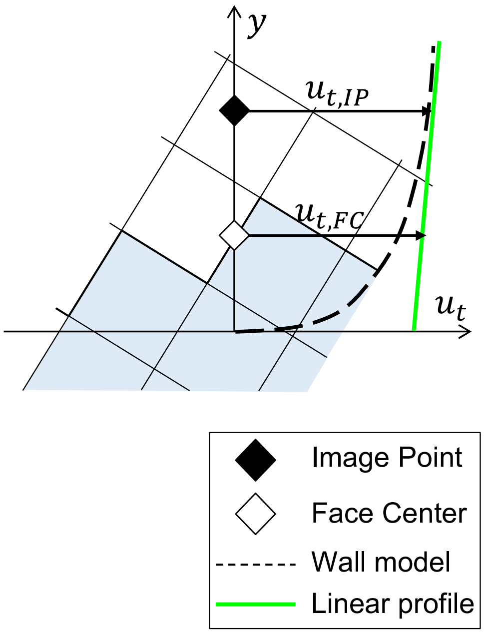

1) Tamaki, Y., Harada, M., and Imamura, T., *AIAA J.*, Vol 55, 2017.

Computational grid

- Unstructured hierarchical Cartesian grid.
- Two grids are used in both steady simulations and unsteady simulations.

	Grid #1 (140M)	Grid #2 (90M)
Total cell number	1.37×10^8	9.02×10^7
Domain size [in.]	2.76×10^4	2.76×10^4
Minimum grid size [in.]	0.281	0.281
Grid size of refinement box [in.]	2.24	4.49
MAC / Minimum grid size	981	981

Computational grid

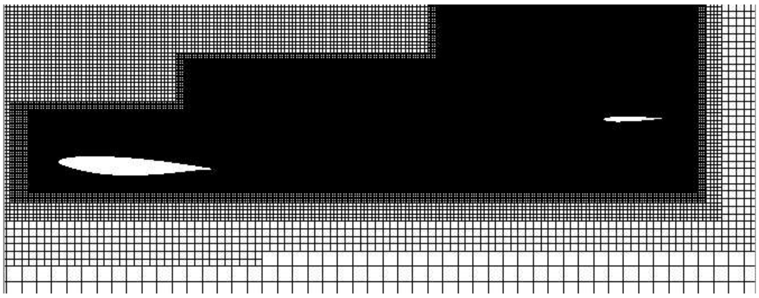

Grid #1 (140M), section YA ($y = 252$ [in.])

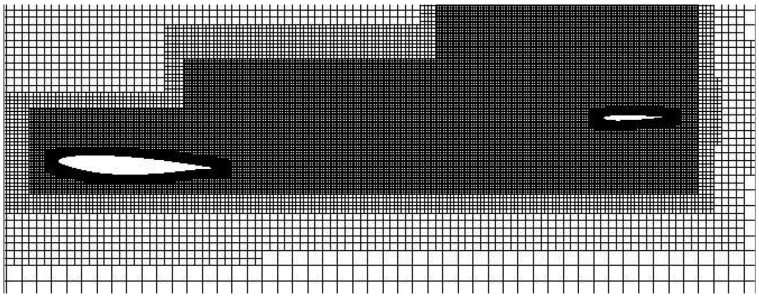

Grid #2 (90M), section YA ($y = 252$ [in.])

Computational grid

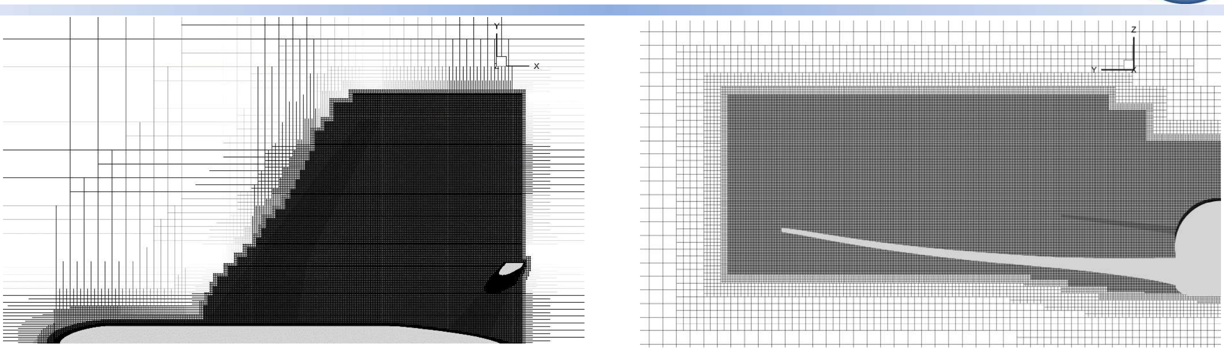

Grid #1 (140M)

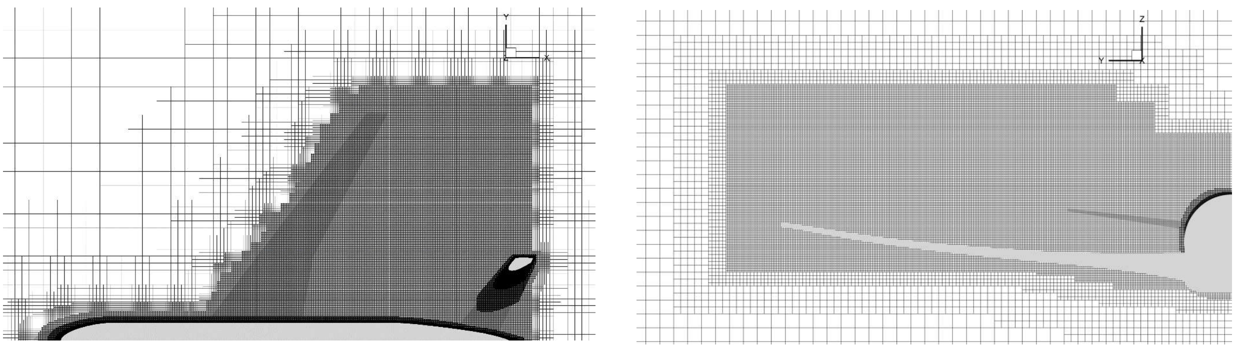

Grid #2 (90M)

Aerodynamic coefficients

- Macro trends match the experiment.
- There is little difference between steady simulation of 140M grid and 90M grid.

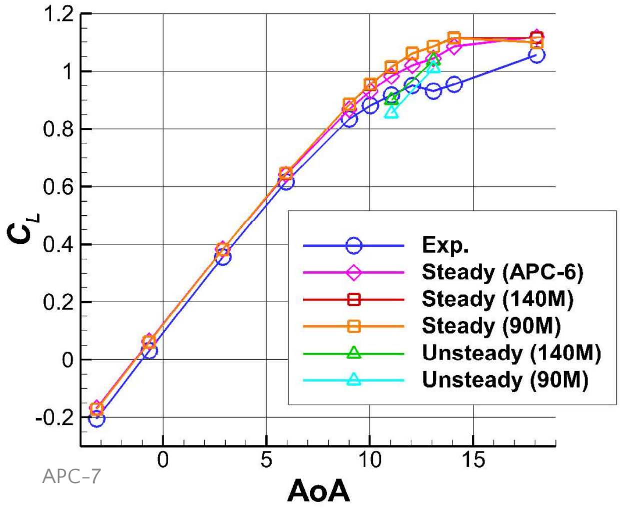

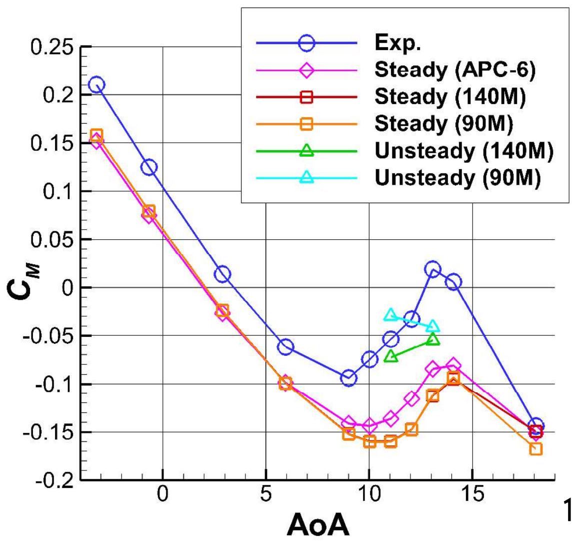

APC-7

11

Aerodynamic coefficients

- Steady simulations overestimate C_L at high AoA.
  - Flow separation seems underestimated.
- Results of unsteady simulations are closer to the experimental values than steady simulations.

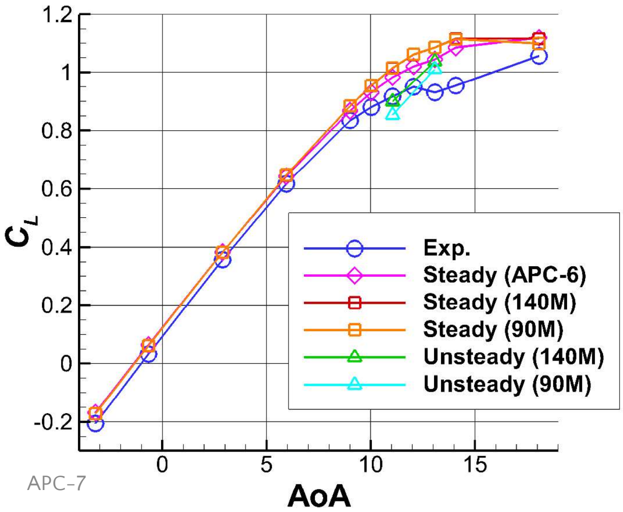

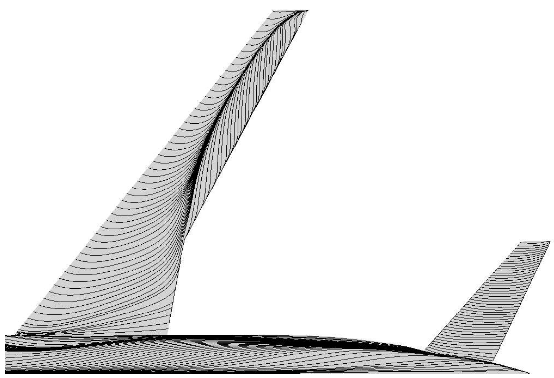

AoA = 13.08 [deg.], Steady (140M)

APC-7

12

Aerodynamic coefficients

- Predicted C_D values are smaller than the experimental values at high AoA.
- C_M values are underestimated.
- Unsteady simulations are closer to the experiment.

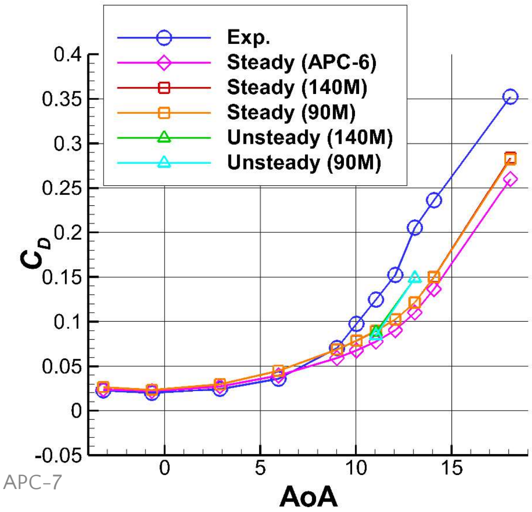

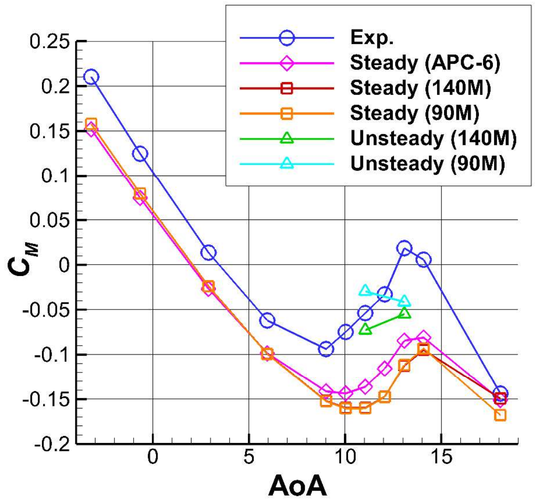

Time history

- Unsteady simulations (DDES) start after 15000 steps of steady simulations (RANS).
- The results from step 45001 to step 90000 are used in this research (about 6.15 sec.).
- $\Delta t = 1.37 \times 10^{-4}$ sec. (both 140M and 90M)

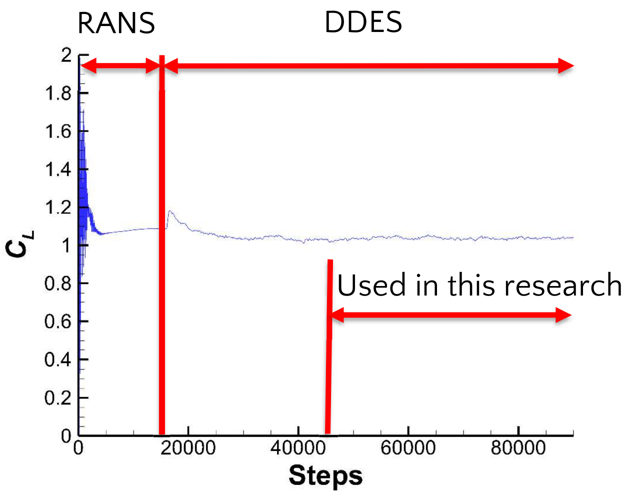

History of C_L, AoA = 11.05 [deg.], Unsteady (140M)

Time history (140M)

- Periodic oscillation is observed at AoA = 11.05 [deg.].
- Flow becomes non-periodic at AoA = 13.08 [deg.].

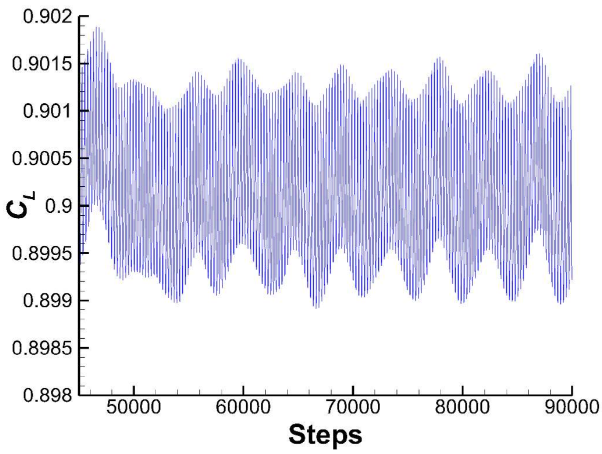

AoA = 11.05 [deg.], Unsteady (140M)

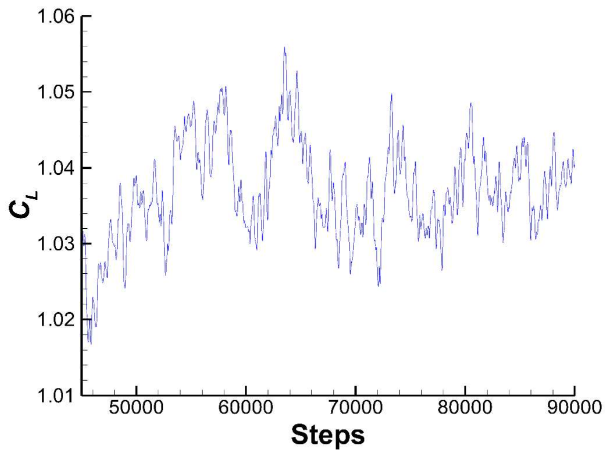

AoA = 13.08 [deg.], Unsteady (140M)

Time history (90M)

- At AoA = 11.05 [deg.], flow has both periodic and non-periodic characteristics.
- At AoA = 13.08 [deg.], flow is non-periodic.

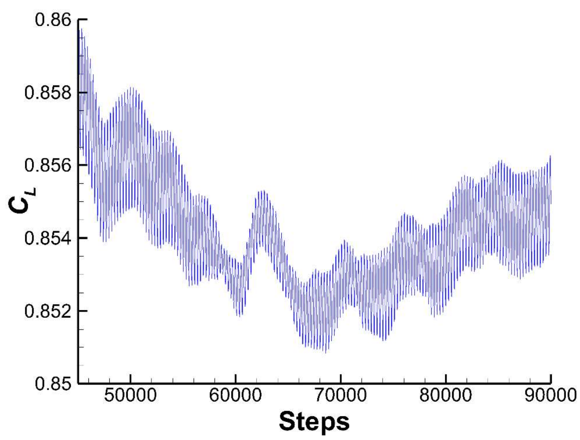

AoA = 11.05 [deg.], Unsteady (90M)

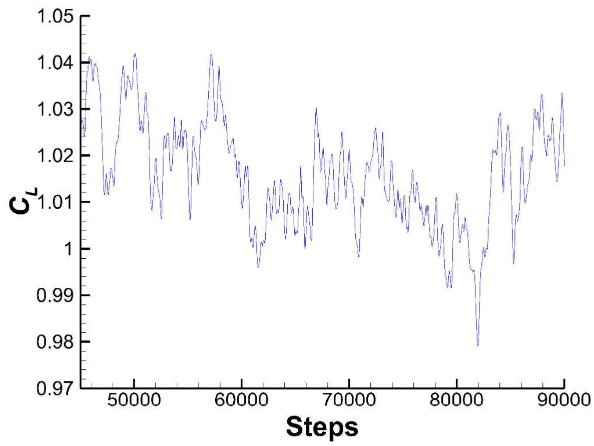

AoA = 13.08 [deg.], Unsteady (90M)

Q criterion

- There is a difference in the wake by AoA and grids.

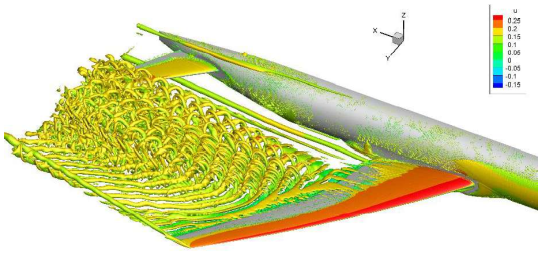

AoA = 11.05 [deg.], Unsteady (140M)

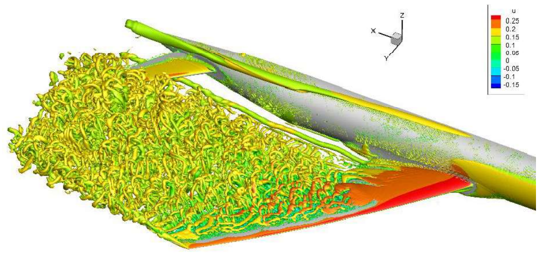

AoA = 13.08 [deg.], Unsteady (140M)

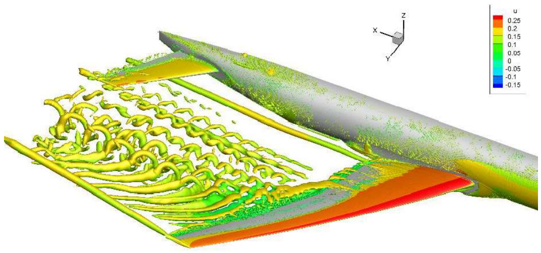

AoA = 11.05 [deg.], Unsteady (90M)

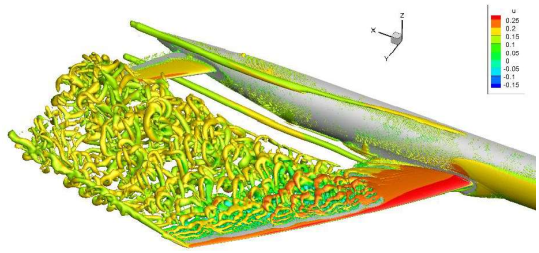

AoA = 13.08 [deg.], Unsteady (90M)

17

Q criterion

- At AoA = 13.08 [deg.], separation occurs from leading edge.

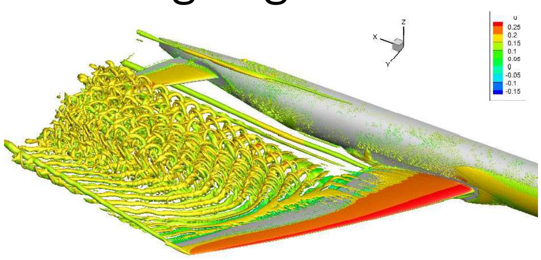

AoA = 11.05 [deg.], Unsteady (140M)

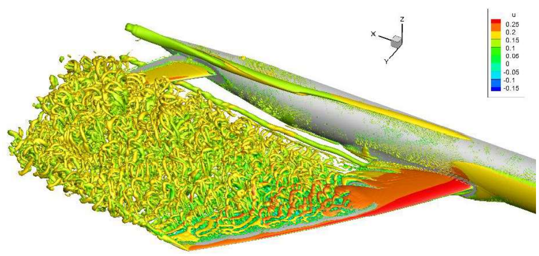

AoA = 13.08 [deg.], Unsteady (140M)

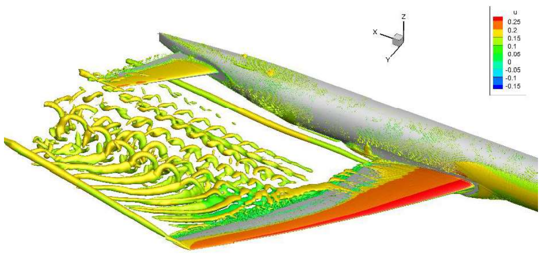

AoA = 11.05 [deg.], Unsteady (90M)

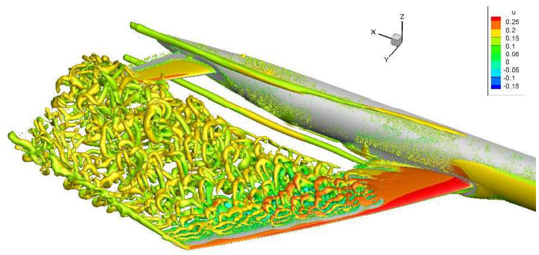

AoA = 13.08 [deg.], Unsteady (90M)

18

Conclusion

- Flow simulations for NASA-CRM at low-speed conditions are conducted by using UTCart and IBM.
  - In many cases, the effect of the difference in the grid width of the wake area is small.
  - The tendency of the aerodynamic coefficients at low angles of attack is consistent with the experimental results.
  - Flow separation at high angles of attack is underestimated in steady simulations.
  - Unsteady simulation improves the predictions of flow separation and aerodynamic coefficients.

APC-7 19

Appendix

東京大学
THE UNIVERSITY OF TOKYO

Coefficients of each component (Unsteady, AoA = 11.05 [deg.])

AoA = 11.05 [deg.]		C_D	C_L	C_M
140M	Main wing	4.79×10^{-2}	7.30×10^{-1}	-1.10×10^{-1}
	Fuselage	3.39×10^{-2}	1.38×10^{-1}	1.70×10^{-1}
	Tail wing	6.67×10^{-3}	3.20×10^{-2}	-1.32×10^{-1}
	Total	8.84×10^{-2}	9.00×10^{-1}	-7.26×10^{-2}
90M	Main wing	4.47×10^{-2}	6.88×10^{-1}	-7.65×10^{-2}
	Fuselage	3.35×10^{-2}	1.36×10^{-1}	1.70×10^{-1}
	Tail wing	6.41×10^{-3}	2.97×10^{-2}	-1.23×10^{-1}
	Total	8.46×10^{-2}	8.54×10^{-1}	-2.94×10^{-2}

Coefficients of each component (Unsteady, AoA = 13.08 [deg.])

AoA = 13.08 [deg.]		C_D	C_L	C_M
140M	Main wing	9.48×10^{-2}	8.29×10^{-1}	-9.41×10^{-2}
	Fuselage	4.50×10^{-2}	1.70×10^{-1}	1.94×10^{-1}
	Tail wing	8.71×10^{-3}	3.77×10^{-2}	-1.54×10^{-1}
	Total	1.49×10^{-1}	1.03	-5.48×10^{-2}
90M	Main wing	9.55×10^{-2}	8.05×10^{-1}	-8.94×10^{-2}
	Fuselage	4.49×10^{-2}	1.69×10^{-1}	1.92×10^{-1}
	Tail wing	8.56×10^{-3}	3.54×10^{-2}	-1.45×10^{-1}
	Total	1.49×10^{-1}	1.01	-4.13×10^{-2}

Computational grid of APC-6(1)

	Steady		unsteady
	w/o sting	w/ sting	
Total cell number	6.85×10^7	8.14×10^7	5.52×10^7
Domain size [in.]	2.76×10^4	2.76×10^4	2.76×10^4
Minimum grid size [in.]	0.421	0.421	0.421
Grid size of refinement box [in.]	3.37	3.37	3.37
MAC / Minimum grid size	655	655	655

1) Yoshinaga, H., Sugaya, K., and Imamura, T., APC-6, 2020